HHS Public Access

Author manuscript

Adv Funct Mater. Author manuscript; available in PMC 2021 April 14.

Published in final edited form as:

Adv Funct Mater. 2020 April 14; 30(15): . doi:10.1002/adfm.201902463.

A Collagen Based Cryogel Bioscaffold that Generates Oxygen for Islet Transplantation

MEHDI RAZAVI[1,2], **ROSITA PRIMAVERA**[1], **BHAVESH D KEVADIYA**[1], **JING WANG**[1], **PETER BUCHWALD**[3], **AVNESH S THAKOR**[1,*]

[1]Interventional Regenerative Medicine and Imaging Laboratory, Stanford University School of Medicine, Department of Radiology, Palo Alto, California 94304, USA

[2]Biionix™ (Bionic Materials, Implants & Interfaces) Cluster, Department of Internal Medicine, College of Medicine, University of Central Florida, Orlando, Florida 32827, USA

[3]Diabetes Research Institute, Miller School of Medicine, University of Miami, Miami, Florida 33136, USA

Abstract

The aim of this work was to develop, characterize and test a novel 3D bioscaffold matrix which can accommodate pancreatic islets and provide them with a continuous, controlled and steady source of oxygen to prevent hypoxia-induced damage following transplantation. Hence, we made a collagen based cryogel bioscaffold which incorporated calcium peroxide (CPO) into its matrix. The optimal concentration of CPO integrated into bioscaffolds was 0.25wt.% and this generated oxygen at 0.21±0.02mM/day (day 1), 0.19±0.01mM/day (day 6), 0.13±0.03mM/day (day 14), and 0.14±0.02mM/day (day 21). Accordingly, islets seeded into cryogel-CPO bioscaffolds had a significantly higher viability and function compared to islets seeded into cryogel alone bioscaffolds or islets cultured alone on traditional cell culture plates; these findings were supported by data from quantitative computational modelling. When syngeneic islets were transplanted into the epididymal fat pad (EFP) of diabetic mice, our cryogel-0.25wt.%CPO bioscaffold improved islet function with diabetic animals re-establishing glycemic control. Mice transplanted with cryogel-0.25wt.%CPO bioscaffolds showed faster responses to intraperitoneal glucose injections and had a higher level of insulin content in their EFP compared to those transplanted with islets alone ($P<0.05$). Biodegradability studies predicted that our cryogel-CPO bioscaffolds will have long-lasting biostability for approximately 5 years (biodegradation rate: 16.00±0.65%/year). Long term implantation studies (i.e. 6 months) showed that our cryogel-CPO bioscaffold is biocompatible and integrated into the surrounding fat tissue with minimal adverse tissue reaction; this was further supported by no change in blood parameters (i.e. electrolyte, metabolic, chemistry and liver panels). Our novel oxygen-generating bioscaffold (i.e. cryogel-0.25wt.%CPO) therefore provides a biostable and biocompatible 3D microenvironment for islets which can facilitate islet survival and function at extra-hepatic sites of transplantation.

[*]**Corresponding Author:** Avnesh S. Thakor, MD PhD, Department of Radiology, Stanford University, 3155 Porter Drive, Palo Alto, CA, 94304, asthakor@stanford.edu, Tel: 650-723-8061, Fax: 650-736-8937.

Keywords

Bioscaffold; Oxygen; Islet Transplantation; Type 1 Diabetes

INTRODUCTION

Although majority of biotechnology research related to islet transplantation has focused on encapsulation strategies,[1–3] there has been a growing interest in creating new biocompatible three-dimensional (3D) structures, known as bioscaffolds.[4–8] Bioscaffolds provide an interesting solution for islet transplantation given that they contain spaces that can accommodate islets while concurrently offering a unique interface which can be modulated to address critical shortcomings faced by islets in the immediate post-transplantation period (i.e. hypoxia).[9] Previous bioscaffolds which have been tested for islet transplantation have mostly been made from synthetic polymers, including poly(lactide-*co*-glycolide),[4] polydimethylsiloxane,[5] poly(D,L-lactide-co-e-caprolactone),[6] poly(ethylene oxide terephtalate)/poly(butylene terephthalate) block copolymer[7] and heparin-binding peptide amphiphiles.[8] Hence, we developed a collagen-based cryogel bioscaffold given that cryogels have enhanced mechanical stability and flexibility compared to traditional hydrogels.[10] Furthermore, our bioscaffold were prepared with interconnected macropores which were large enough to accommodate islets as well as facilitate islet migration throughout its structure; the latter is important as it improves islet survival and function by preventing clumping and ensuring a more even distribution of islets.[11] Collagen was used as our base biopolymer given that it is a primary component of the extracellular matrix (ECM) of connective tissue, is readily available, has a fibril architecture similar to natural tissues and has reduced biodegradability.[12,13]

Although previous bioscaffolds have been functionalized with exogenous growth factors (i.e., exendin-4,[14] insulin-like growth factor-1,[14] transforming growth factor-beta 1,[15] ECM,[16] vascular endothelial growth factor[8] and fibroblast growth factor-2[8]) to improve islet survival and function, they have not addressed the issue of providing islets with the most essential nutrient they require in the immediate post-transplantation period – oxygen. Indeed, without any oxygen supplementation, there is substantial cellular dysfunction and death of islets within bioscaffolds as a result of low oxygen tensions.[17,18] One approach to address this issue has been to use oxygen generating biomaterials (i.e. using calcium peroxide (CPO) contained within a PDMS disk - OxySite[17]). Although promising, the OxySite disk cannot be incorporated into the structure of a 3D bioscaffold; in turn, this results in a non-uniform delivery of oxygen to islets seeded into bioscaffolds that are transplanted with the disk.[17]

Hence, in the present study we decided to incorporate an oxygen generating biomaterial (i.e. CPO) into the matrix of our macroporous collagen-based cryogel bioscaffold[19], such that oxygen can be uniformly given to all islets seeded into the bioscaffold. We chose CPO given its ability to generate and release oxygen as it gets hydrolyzed in the presence of water[20,21] (Figure 1a). However, exposure of CPO to aqueous solution generates reactive oxygen species (ROS) such as hydrogen peroxide (H_2O_2). Although ROS have an important role in

cell signaling and homeostasis, in excess they cause oxidative stress which can have a negative effect on islet survival and function, especially since islets themselves have limited antioxidant defense mechanisms.[22] In fact, H_2O_2 has been shown to decrease the ATP/ADP ratio, increase intracellular Ca^{2+}, and inhibit glucose-stimulated insulin secretion from isolated islets.[23] Hence, elevation of ROS can cause damage to structural proteins, enzymes and membranes, which, in turn, can lead to the spontaneous destruction of β-cells within pancreatic islets.[24] This study therefore optimized the incorporation of CPO into the collagen matrix to enable the release of oxygen in a sustained and controlled manner over the time required for transplanted islets to establish their own blood supply and hence their own supply of oxygen, while also producing the lowest amount of ROS. To test this bioscaffold *in vivo*, we transplanted it into the epididymal fat pad (EFP) of diabetic mice; this location in mice is representative of the omentum in humans[25] which is an extra-hepatic site currently being tested in clinical trials for islet transplantation.[26]

MATERIALS AND METHODS

Bioscaffold Synthesis and Characterization

Bioscaffolds were synthesized from collagen and CPO using a cryogelation technique (Figure 1b–c). Porosity, density, structure, chemical and mechanical properties of synthesized bioscaffolds were then characterized (See Supplemental Material). Oxygen release from bioscaffolds (discs measuring 0.5mm thick × 1mm diameter) was measured using a Dissolved Oxygen (DO) Meter (YSI™ Pro2030, USA; DO range of 0–1.5mM) connected to a YSI™ 2003 Pro Series Polarographic DO Sensor. The DO meter was calibrated using distilled water (DO = 0.2 mM) as per the manufacturer's guidelines. Bioscaffolds were immersed in a sealed vial that contained PBS (10mL) and incubated in a humidified incubator under normal conditions (0.2 mM (20%) O_2 and 5% CO_2) at 37 °C. Measurements were collected at day 1, 2, 3, 6, 9, 14 and 21. Each measurement was collected for 5min. Control experiments were also performed by measuring the change in DO in the absence of bioscaffolds by using sealed vials containing PBS alone. The difference between the DO of the PBS solution alone and PBS solution which contained bioscaffolds was then reported as the oxygen released from bioscaffolds. Since the PBS solution was refreshed every day, results was therefore reported as the oxygen released per day (mM/day). Reactive oxygen species (ROS) were measured at day 7 using a fluorometric assay using 2′,7′-Dichlorofluorescin diacetate (DCFH-DA; Sigma–Aldrich) (See Supplemental Material). All characterizations were performed on the same size (discs measuring 5mm thick × 10mm diameter) and weight (40mg) of cryogel-CPO bioscaffolds in their dry state.

Multiphysics Computational Modeling

To estimate the effect of oxygen released form our cryogel-CPO bioscaffolds on the survival and function of islets, we created computational models using a previously calibrated quantitative model for avascular pancreatic islets.[27,28] In brief, a total of four concentrations were used for convective and diffusive mass transport modeling, with their corresponding equations (application modes): glucose, oxygen, 'local' and released insulin

(c_{gluc}, c_{oxy}, c_{insL}, c_{ins}). Diffusion of all species was assumed to be governed by the generic diffusion equation (Eq. 1) in its non-conservative formulation (incompressible fluid):

$$\frac{\partial c}{\partial t} + \nabla \cdot (-D\nabla c) = R - \boldsymbol{u} \cdot \nabla c \quad \text{(Eq. 1)}$$

where c denotes the concentration [mol·m^{-3}], D the diffusion coefficient [m^2·s^{-1}], R the reaction rate [mol·m^{-3}·s^{-1}], **u** the velocity field [m·s^{-1}], and ∇ the standard *del* (*nabla*) operator $\left(\nabla \equiv \boldsymbol{i}\frac{\partial}{\partial x} + \boldsymbol{j}\frac{\partial}{\partial y} + \boldsymbol{k}\frac{\partial}{\partial z}\right)$. All consumption and release rates were assumed to follow Hill–type dependence on the local concentrations (Eq. 2):

$$R = f_H(c) = R_{max}\frac{c^n}{c^n + C_{Hf}^n} \quad \text{(Eq. 2)}$$

Here, R_{max} denotes the maximum reaction rate [mol·m^{-3}·s^{-1}], C_{Hf}, the concentration corresponding to half-maximal response [mol·m^{-3}], and n, the Hill slope characterizing the shape of the response. Diffusion coefficients and parameter (R_{max}, C_{Hf}, and n) values for all species (i.e. insulin, glucose, and oxygen) used were derived from a previously developed model.[28] The model is implemented in COMSOL Multiphysics (COMSOL Inc., Burlington, MA) and solved as a time-dependent (transient) problem with intermediate time-steps for the solver.

The geometry used (Figure 2) represents a small cross section of a typical bioscaffold and assumes a 3D porous structure resembling that of our cryogel-CPO bioscaffold, with 300μm pore size, seeded with representative islets with diameters of 120 and 150μm at densities resembling those of our actual bioscaffolds. Mesh and boundary conditions used are as described before (i.e., COMSOL's predefined 'finer' mesh size).[27,28] As boundary conditions, fixed concentrations were used for the top and bottom (as those are in contact with surrounding tissues), and symmetry conditions were used for the left and right borders (as the model represents only a small part of a whole bioscaffold). Cryogel-CPO bioscaffolds were assumed to be in an aqueous media at physiological temperature (37°C) with an oxygen concentration of c_{oxy} = 0.050mol·m^{-3} (mM) corresponding to typical tissue oxygenation,[29–32] and a glucose concentration of 8mM corresponding to normal glucose levels in mice.[33] The oxygen generation rate was assumed to be constant and incorporated this into the model as a continuous release (reaction rate per unit volume) across the entire bioscaffold; the rate used was 0.01 M/m^3/s, which corresponds to a rate of 0.1 mM/day/bioscaffold for the bioscaffold (based on its volume).

In Vitro Interactions of our Bioscaffold with Pancreatic Islets

Islets were hand-picked and seeded into sterilized bioscaffolds, achieving a density of 20 islets in 200 μL complete medium per bioscaffold; these were then placed within each well of a 96-well plate. Islets seeded into bioscaffolds were cultured in a humidified incubator under normal conditions (0.2 mM (20%) O_2 and 5% CO_2) at 37 °C. All experiments were performed in n=5 on following experimental groups: 1) islets alone or islets seeded into 2) cryogel, 3) cryogel-0.25wt.%CPO, 4) cryogel-0.5wt.%CPO, and 5) cryogel-1wt.%CPO bioscaffolds. The viability and function of islets were determined using live/dead, 3-(4,5-

Dimethylthiazol-2-yl)-2,5-diphenyltetrazolium bromide (MTT) and glucose stimulated insulin secretion (GSIS) assays. Islets were also visualized with a confocal microscope and SEM (See Supplemental Material). All in vitro experiments were performed on the same size (discs measuring 0.5mm thick × 1mm diameter or 0.4mm^3 volume) bioscaffolds in their dry state.

In Vivo Interactions of our Bioscaffold with Pancreatic Islets

All procedures were performed in accordance with the regulations approved by the Institutional Animal Care and Use Committee (IACUC) of Stanford University. Following islet transplantation into both EFPs of diabetic mice, metabolic assessment which included non-fasting blood glucose measurements and Intraperitoneal Glucose Tolerance Tests (IPGTT) were performed in conscious mice at the indicated time points. At day 30 post-transplant, mice were euthanized and serum and tissue (i.e. the EFP with or without bioscaffolds) samples collected to determine insulin levels (insulin ELISA kit; Mercodia). In addition, the EFP tissue was processed for histological (i.e. fixed in 4% paraformaldehyde, dehydrated with graded ethanol solutions, embedded in paraffin and sliced with a microtome) and/or molecular (i.e. tissues stored at −80°C for subsequent processing to determine levels of cytokines) analyses. A total of 5 experimental groups were used (n=8 animals per group): Group 1: Mice transplanted with islets only; Group 2: Mice transplanted with islets seeded into cryogel alone bioscaffolds; Group 3: Mice transplanted with islets seeded into cryogel-0.25wt.%CPO bioscaffolds; Group 4: Normal non-diabetic mice; Group 5: Diabetic mice which did not receive any islet transplantation. In our study, these groups are called as islets only, islets seeded into cryogel bioscaffolds, islets seeded into cryogel-0.25wt.%CPO bioscaffolds, normal mice and diabetic mice, respectively (See Supplemental Material). All in vivo experiments were performed on the same size (discs measuring 0.5mm thick × 3.5mm diameter or 5mm^3 volume) bioscaffolds in their dry state. For both *in vitro* and *in vivo* experiments, the same islet loading density in bioscaffolds (i.e. 50 islets/mm^3) was used.

Assessment of Hypoxia Induced Factor (HIF) Expression

To assess HIF-1 expression in EFPs containing islets seeded into our cryogel bioscaffolds, western blot analysis was performed as previously described[34]. In brief, islets were lysed in radioimmunoprecipitation assay buffer (RIPA buffer; 50mM Tris, 0.3M NaCl, 0.5% Triton X, pH 7.5) in the presence of protease inhibitors (Sigma Aldrich, USA) and centrifuged at 18,500g for 15min. The pellet was then discarded and the supernatant was kept for further analysis. Protein concentration was measured using a bicinchoninic acid (BCA) assay kit (Thermo scientific, USA). Loading buffer (Biorad, USA) was added to the samples before loading an equivalent microgram of proteins for each sample on precast gel from Bio-Rad. Protein bands were then transferred onto a nitrocellulose membrane using a Bio-Rad trans-blot turbo system. Expression levels of hypoxia induced factors (HIF) include HIF1β, HIF1α, and HIF2α proteins were measured with respective antibodies for HIF1β, HIF1α, and HIF2α (1:200 dilution, all from Cell Signaling Technology (USA)). An anti-βactin antibody was also used as a loading control (dilution: 1:10000, Santa Cruz Biotechnology, USA). Antibody incubations and developments were performed using Chemiluminescence kit and ChemiDoc (Bio-Rad, USA). Goat anti-mouse horseradish peroxidase (1:5000; Santa

Cruz Biotechnology) was used as a secondary antibody and incubated for 1h at room temperature. Specific proteins were detected by chemiluminescent methods while protein abundance on western blots was quantified by densitometry using Image lab software (Bio-Rad, CA).

Bioscaffold Biodegradability and Biocompatibility

Biodegradability: Cryogel-0.25wt.%CPO bioscaffolds were weighed (dry weight: W_{d1}) and then incubated in PBS at 37°C for 12 weeks. Every week, bioscaffolds were removed from PBS, dried overnight and re-weighed (dry weight (W_{d2})). The degree of bioscaffold biodegradation was calculated as follows: $((W_{d1}-W_{d2})/W_{d1} \times 100)$.

Biocompatibility: Cryogel-0.25wt.%CPO bioscaffolds were implanted into the EFP and subcutaneous tissue of C57/B6 mice. After 6 months, mice were sacrificed and the EFP and subcutaneous tissue containing the implanted bioscaffolds were harvested for macroscopic and microscopic (i.e. histology with H&E) examination, specifically looking at the bioscaffold and surrounding tissue. Blood samples were also collected for routine analysis (i.e. electrolyte, metabolic, chemistry, and liver panels).

Statistical Analysis

All experiments were performed in n=5 for *in vitro* or n=8 for *in vivo*, and results were expressed as mean±standard error of the mean. Statistical analysis of all quantitative data was performed using a one or two-way ANOVA (Analysis of Variance) with post-hoc Tukey test (Astatsa.com; Online Web Statistical Calculators, USA) with any differences considered statistically significant when $P<0.05$.

RESULTS

Bioscaffold Synthesis and Characterization

Synthesized cryogel bioscaffolds measured 10mm (diameter) × 5mm (thickness) corresponding to a volume of 393±1mm^3 with a porosity of 75±3% and density of 0.03±0.01mg/mm^3. Cryogel-CPO bioscaffolds can release oxygen over 21 days, with the rate of oxygen release significantly increasing as the concentration of CPO increases from 0.25 to 1wt.% ($P<0.05$). For cryogel-0.25wt.%CPO the rate of oxygen released was 0.21±0.02 mM/day at day 1, 0.19±0.01 mM/day at day 6, 0.13±0.03 mM/day at day 14, and 0.14±0.02 mM/day at day 21 (Figure 1d). However, this was accompanied by an increase in ROS production from cryogel-CPO bioscaffolds. Furthermore, increasing the concentration of CPO from 0.25 to 1wt.% within bioscaffolds resulted in a significant increase in ROS production (0.36±0.02 to 1.52±0.01 absorbance, respectively; $P<0.05$; Figure 1e).

The addition of CPO changed the bioscaffold porosity and density to 70±5% and 0.04±0.01mg/mm^3, respectively (Figure 1f). Micro (μ)-CT images demonstrated the shape and distribution of pores within the 3D structure of bioscaffolds (Figure 1g). The pore size, measured in 5 different bioscaffolds at 5 random locations, fall into 2 groups: big pores=300±50μm and small pores=30±10μm (Figure 1h). Following incorporation of CPO

into cryogel bioscaffolds, CPO particles were detected using SEM (Figure 1i) and confirmed using XPS (Figure 1j) and EDS analysis (Figure 1k).

Using the compression test, all bioscaffolds showed elastic behavior until 60% compression of their length. Thereafter, the uni-axial stress was transferred to the plastic region. Cryogel alone bioscaffolds showed an elastic modulus of 4.9±0.6KPa, yield strength of 2.4±0.3KPa and compression strength of 4.8±0.5KPa. Incorporation of CPO into the bioscaffold matrix resulted in a significant increase in elastic modulus, yield strength and compression strength which was proportional to the concentration of CPO from 0.25 to 1wt.% (Figure 1l; $P<0.05$). Moreover, cryogel-CPO bioscaffolds could recover to their original shape after removing the compression loads (Figure 1m).

Multiphysics Computational Modeling

Computational modeling of islet oxygen consumption and insulin secretion was performed with a local concentration-based model implemented using a finite element method (FEM). Oxygen concentrations are color-coded from blue for high to red for low with white indicating levels that are below the critical concentration of oxygen ($c_{oxy} < c_{crit}$) for islet survival. Insulin secretion rates per unit volume within the islets are shown color-coded from black for high to white for zero with white indicating levels that are below the oxygen concentration needed for insulin production[27]. In 2D cross-sections, the core of islets seeded into our cryogel bioscaffolds is predicted to be not only necrotic if there is no oxygen support (Figure 2a) but also non-functional (i.e. unable to produce insulin in response to a glucose challenge) (Figure 2b) due to the diffusion limitations in avascular islets, where there is a lack of vascularization. However, oxygen released from our cryogel-0.25wt.%CPO bioscaffolds, even at levels corresponding to those released 2–3 weeks after transplantation, is predicted to overcome these problems and, hence, provide improved islet viability and function (Figure 2c,d). When the interaction of islets with our bioscaffold was experimentally tested, our results matched the FEM model - the oxygen released from our cryogel-0.25wt.%CPO bioscaffold improved the viability of islets when compared to islets that were seeded into cryogel alone bioscaffolds (90±4 vs 50±6% live cells at day 7; $P<0.05$; Figure 2e–f)

In Vitro Interactions of our Bioscaffold with Pancreatic Islets

Islets seeded into cryogel-0.25wt.%CPO bioscaffolds were evenly distributed as demonstrated by their presence on the top (Figure 3a–b) as well as the center of the bioscaffold (Figure 3c–d) with no clumping noted. In contrast, islets cultured in cell culture plates (i.e. control group) demonstrated aggregation/clumping after 7 days of culture (Figure 3e–f). Compared to the control group, islets seeded into bioscaffolds that incorporated CPO demonstrated a significant increase in the percentage of live cells (determined using the Live/Dead assay, $P<0.05$, Figure 3g–h), a significantly greater viability (determined using the MTT assay, $P<0.05$; Figure 3i), and improved functionality - insulin secretion (determined using a GSIS assay, $P<0.05$; Figure 3j–k). These effects were greatest for islets seeded into cryogel-0.25wt.%CPO bioscaffolds, which demonstrated an increase in live cells (90±7% vs. 35±3%; $P<0.05$), cell viability (islet viability ratio: 2.4±0.1 vs. 1.0±0.1; $P<0.05$), and insulin secretion (low glucose stimulation: 0.63±0.13 vs. 0.50±0.01ng/mL;

high glucose stimulation: 2.10±0.05 vs. 1.23±0.14ng/mL; P<0.05; Figure 3j) when compared to the control group. Calculation of the insulin stimulation index (SI: ratio of insulin secretion from high glucose stimulation relative to basal conditions) also showed a significant increase for cryogel-0.25wt.%CPO bioscaffolds compared to the control group (3.31±0.09 vs. 2.45±0.27; P<0.05; Figure 3k)

In Vivo Interactions of our Bioscaffold with Pancreatic Islets

Experimental details of our *in vivo* experiment and transplantation procedure are outlined in Figure 4a–d. At sacrifice, cryogel-0.25wt.%CPO bioscaffolds were tightly wrapped within the EFP (Figure 4c) and following their extraction were noted to be engrafted within the fat tissue with no evidence of adhesions/fibrous bands.

Following STZ treatment, all animals became hyperglycemic (non-fasting blood glucose values increasing from 128±8mg/dL (day −2) to 538±25mg/dL (day 0); Figure 4e). Compared to all experimental groups that received islet transplantation, immediate and sustained reversal of hyperglycemia was only observed in mice which received islets seeded in cryogel-0.25wt.%CPO bioscaffolds. At day 1 post-transplantation, mice that received islets seeded in cryogel-0.25wt.%CPO bioscaffolds demonstrated significantly lower non-fasting blood glucose values compared to mice transplanted with islets only (221±61 vs. 390±55mg/dL; P<0.05; Figure 4e). This difference was sustained throughout the course of the study in animals which had received islets seeded into cryogel-0.25wt.%CPO bioscaffolds with these animals demonstrating glycemic control with their non-fasting blood glucose values, from day 1–30, now being similar to their baseline/pre-diabetic values (P>0.05; Figure 4e). Animals which had received islets seeded into cryogel-0.25wt.%CPO bioscaffolds showed a significantly lower non-fasting blood glucose values from day 1 to 30 (P<0.05; Figure 4e) compared to mice transplanted with islets only and mice that received islets in cryogel alone bioscaffolds (except at day 6, 9, 11, 12, 18, 21, and 25). For mice that received islets only or islets seeded into cryogel bioscaffolds alone, only 9% and 25% of animals become normoglycemic, respectively. However, for animals which received islets seeded into cryogel-0.25wt.%CPO bioscaffolds, the percentage of animals that exhibited normoglycemia in the first week following transplantation was 65%; this value is significantly higher than mice which received islets only or islets seeded into cryogel bioscaffolds alone (P<0.05; Figure 4f).

At day 0, all mice weighed 18±1g. Following transplantation, the body weight of all mice increased; however, this increment was significantly higher for mice transplanted with islets seeded into cryogel-0.25wt.%CPO bioscaffolds than in mice that received islets seeded into cryogel alone bioscaffolds (P<0.05) or islets only (P<0.05). At day 30 post-transplantation, there was no significant difference between the body weight of mice that received islets seeded into cryogel-0.25wt.%CPO bioscaffolds compared to normal mice (22.6±0.8 vs. 22.4±0.5; P>0.05). In contrast, the body weight of diabetic mice (i.e. non-transplanted mice) significantly reduced from 17.5±0.2 to 15.1±1.1g after 30 days (Figure 4g, P<0.05).

For all groups, there was an increase in the change in blood glucose level relative to baseline levels (i.e. 0min) following intraperitoneal glucose administration with a peak-value seen at 30min. Mice that received islets seeded into cryogel-0.25wt.%CPO bioscaffolds

(256±13mg/dL) or cryogel alone bioscaffolds (294±22mg/dL) showed a similar peak value compared to normal mice (252±10mg/dL; P>0.05), however, this value was significantly lower than mice which received islets only (331±23mg/dL) or diabetic mice (344±22mg/dL; P<0.05; Figure 4h). The area under the curve ($AUC_{0–120min}$) for mice that received islets seeded into cryogel-0.25wt.%CPO bioscaffolds (11,657±1,440mg/dL.min) was significantly lower compared to mice that received islets seeded into cryogel alone bioscaffolds (29,551±3,018mg/dL.min), islets only (31,591±3,177mg/dL.min) and diabetic mice (36,101±2,525mg/dL.min; P<0.05) with no change compared to normal mice (10,320±971 mg/dL.min; P>0.05; Figure 4i). The glucose clearance rate (i.e. the slope of blood glucose change from 30–120min) showed that mice that received islets seeded into cryogel-0.25wt.%CPO bioscaffolds (2.78±0.05mg/dL/min) had a significantly faster glucose clearance compared to mice that received islets seeded into cryogel alone bioscaffolds (2.15±0.19 mg/dL/min), islets only (2.02±0.23 mg/dL/min) and diabetic mice (1.82±0.17 mg/dL/min; P<0.05) with no change compared to normal mice (2.78±0.02 mg/dL/min, P>0.05; Figure 4j).

In animals which were transplanted with islets alone into the EFP, at the time of sacrifice there were few intact islets visualized; furthermore, these remaining islets had lost their spherical morphology and intrinsic architecture and were collapsed with insulin staining cells now noted to be dispersed throughout the EFP rather than localized to discrete islet structures. When islets were transplanted into bioscaffolds, they could be easily identified within the bioscaffolds pores (red arrows). Islets which were seeded into cryogel-0.25wt.%CPO bioscaffolds, were found on histological analysis to be significantly greater in number compared to animals which received islets seeded into cryogel alone bioscaffolds or islets only (total islet area: 0.68±0.17 vs. 0.24±0.06 mm^2 or 0.08±0.03 mm^2, respectively, P<0.05; Figure 5a). Transplanted islets seeded into cryogel-0.25wt.%CPO or cryogel alone bioscaffolds retained their native size, spherical morphology and maintained their intrinsic architecture with β cells (positive insulin staining) located in the center of the islets. In keeping with this, there was significantly higher insulin staining within islets seeded into cryogel-0.25wt.%CPO compared to cryogel alone bioscaffolds (percentage of insulin per islet: 76.6±11.2 vs. 35.5±12.3%, respectively; P<0.05; Figure 5a). Transplanted islets seeded into cryogel-0.25wt.%CPO bioscaffolds also demonstrated reduced inflammation as evidenced by a reduction in the presence of TNF-α compared to islets only (2.1±0.2 vs. 16.2±3.3%; P<0.05; Figure 5a and Figure S7).

The levels of insulin in the blood was significantly higher for mice that received islets seeded into a cryogel-0.25wt.%CPO bioscaffold or a cryogel alone bioscaffold compared to mice transplanted with islets only (2.14±0.57 or 1.38±0.35 vs. 0.36±0.12ng/mL, P<0.05) with no significant difference seen between cryogel-0.25wt.%CPO and cryogel alone bioscaffolds (2.14±0.57 vs. 1.38±0.35ng/mL; P>0.05; Figure 5b). Similar results were also seen for the levels of insulin in the EFP tissue (0.76±0.05 or 0.59±0.03 vs. 0.44±0.08μg/mL; P<0.05; Figure 5c). In addition, the EFP tissue from animals which had received an islet transplant with cryogel-0.25wt.%CPO bioscaffolds demonstrated up-regulation of macrophage inflammatory protein-1-alpha and beta (MIP-1α: +6.08±1.33 and MIP-1β: +4.84±1.59 fold change), interferon gamma-induced protein-10 (IP-10: +1.80±0.42 fold change), interleukin-6 (IL6: +1.23±0.05 fold change) and down-regulation of interleukin 9

(IL9: −0.52±0.09 fold change), lipopolysaccharide-induced CXC chemokine (LIX: −0.53±0.1 fold change), and tumor necrosis factor-alpha (TNF-α: −0.55±0.13 fold change) when compared to the control animals which received islets only ($P<0.05$; Figure 5d). Differences were also noted in the expression of interleukin-22 (IL-22), leukemia inhibitory factor (LIF), interleukin-28 (IL28) and TNF-α within the EFP tissue of animals which received islets seeded into cryogel-0.25wt.%CPO and cryogel alone bioscaffolds ($P<0.05$).

Assessment of Hypoxia Induced Factor (HIF) Expression

Western blot analysis demonstrated that compared to both islets only and cryogel alone bioscaffolds, when islets seeded into our cryogel-0.25wt.%CPO bioscaffolds and transplanted into the EFP of diabetic mice, EFPs showed a significantly lower expression of HIF1α (0.65±0.11 vs 1.02±0.65 and 0.93±0.01 relative expression, respectively; $P<0.05$; Figure 6). EFPs containing islets seeded into our cryogel-0.25wt.%CPO bioscaffolds also showed a significantly lower expression of HIF2α when compared to group in which the EFPs contained transplanted islets only (0.12±0.18 vs 0.64±0.03 relative expression; $P<0.05$; Figure 6,).

Bioscaffold Biodegradability and Biocompatibility

After 3 months incubation in PBS, the biodegradation degree of cryogel-0.25wt.%CPO bioscaffolds was 10.30±0.27% (Figure 7a). At 6 months post-implantation, cryogel-0.25wt.%CPO bioscaffolds (red arrows) were well integrated into the EFP or subcutaneous tissue with clear surface boundaries at the bioscaffold-tissue interfaces. Histological images show some foreign body reaction (FBR) inside the bioscaffold pores as demonstrated by the formation of fibrous tissue. However, there was minimal FBR at the host-bioscaffold junction (Figure 7b). Blood analysis at 6 months demonstrated no significant elevation in any parameter with average values from all animals contained within their respective normal range[35,36] (Figure 7c).

DISCUSSION

It is well established that oxygen is critical for islet survival and this is supported by data showing the high metabolic activity of islets as well as the disproportionate increase in oxygen consumption of islets compared to the neighboring exocrine pancreatic tissue.[37,38] However, the process of islet transplantation substantially reduces the ability of islets to obtain a consistent and reliable supply of oxygen given that they (i) get de-vascularized during their isolation process and hence have to rely on the diffusion of oxygen from the host tissue in the short term and (ii) are delivered into a relative hypoxic environment during portal venous infusion into the liver. Hence, we sought to address this shortcoming by enabling our cryogel bioscaffold[39] to release oxygen, in a sustained and controlled manner, over the time frame required for transplanted islets to develop their own dedicated blood supply (i.e. 2–3 weeks).[40]

Although, most CPO based oxygen releasing systems have used hydrophobic polymers, such as PDMS[17] or polyurethane (PU)[41], we used collagen (i.e. a naturally occurring hydrophilic system), given its excellent biocompatibility and low immunogenicity.[42] As

collagen is a component of the ECM,[9] islets that are seeded into our bioscaffold will therefore be exposed to a microenvironment similar to that of the native pancreas which, in turn, helps to maintain their function as well as regulate their cellular activities.[43] This is supported by our *in vitro* (MTT, live/dead and GSIS assays) and *in vivo* (metabolic analysis) data showing that bioscaffolds made from cryogel alone improved islet function and viability when compared to islets alone. Similar results showing improvement in islet function have been reported using bioscaffolds that have been either coated with ECM components[44] or those using ECM derived from lung tissue.[45,46] However, to minimize the effect of any ROS produced from our hydrophilic collagen-based cryogel bioscaffold, we tested different concentrations of CPO, and found that 0.25wt.% concentration of CPO produced the most desirable results; these bioscaffolds generated biologically relevant concentrations of oxygen[17,27] over 21 days while also producing the lowest amount of ROS compared to bioscaffolds which incorporated higher concentrations of CPO.

Recently, cryogels have gained interest due to their larger interconnected macropores (i.e. super-macropores) and enhanced mechanical stability compared to traditional hydrogel constructs[19,47,48]. Cryogels are synthesized using the process of cryogelation, which involves a cycle of freezing, storage of the solvent in the frozen state, followed by defrosting. In this technique, the dissolved solutes (monomers or polymer precursors) are concentrated in small unfrozen regions. After synthesis, the melting of these solvent ice crystals, which serve as porogens (i.e. niduses for pore formation), leaves behind a system of large interconnected pores[47,48]. In our study, the interconnected macropores within our cryogels enabled islets to be evenly distributed throughout its 3D matrix. In turn, this prevented islets from clumping resulting in their improved function and survival, as similarly observed in previous studies.[49–51]

The macropores within our bioscaffolds also enabled islets to be evenly distributed throughout its 3D matrix. In turn, this prevented islets from clumping resulting in their improved function and survival, as similarly observed in previous studies.[49–51] In addition, islets seeded within our bioscaffolds were able to maintain their native rounded morphology, size and architecture, all of which have been shown to play a crucial role in their function and outcome following transplantation.[51] Studies have also shown that the pores of a bioscaffold not only guarantee islet retention and separation within the construct, but also allows mass transfer of metabolites and ingrowth of blood vessels, resulting in an intra-islet vascular density that is comparable to native islets.[7,9,52] Furthermore, compression testing revealed instant shape recovery of our cryogel-CPO bioscaffolds after unloading. Potential pre-clinical and clinical sites for the implantation of our cryogel-0.25wt.%CPO bioscaffold include the omentum or the subcutaneous space; in these locations, bioscaffolds could be subjected to complex and repeated compression loads. Our results show the elasticity of our bioscaffold in such cases given that compression tests showed recovery of our bioscaffold to its original shape following removal of different compressive stresses. This high flexibility helps to prevent pore collapse during bioscaffold implantation, thereby providing a mechanically stable microenvironment for islets.

To enable our bioscaffold to release oxygen, we incorporated a biocompatible solid peroxide into the matrix of our bioscaffold. Upon exposure of CPO to water, hydrogen peroxide

(H_2O_2) is formed (reaction 1) which subsequently decomposes to generate oxygen (reaction 2) in a sustained-release manner.[20,21]

$$CaO_2(s) + 2H_2O(l) \rightarrow Ca(OH)_2(s) + H_2O_2(l) \quad \text{(reaction 1)}$$

$$2H_2O_2(l) \rightarrow 2H_2O(l) + O_2(g) \quad \text{(reaction 2)}$$

The beneficial effects of CPO on pancreatic islets have been reported by Pedraza and colleagues who concluded that incorporation of CPO into polydimethylsiloxane (PDMS) non-porous disks (i.e. OxySite disk) resulted in a sustained generation of oxygen and elimination of hypoxia-induced cellular dysfunction. In turn, this resulted in normalization of islet metabolic function and glucose-dependent insulin secretion.[20] However, the main advantage of our bioscaffold approach, over this and other approaches to deliver oxygen to islets,[17,18] is the ability of our bioscaffold to evenly distribute the supply of oxygen to all the islets seeded into the bioscaffold given that CPO had been integrated into the actual bioscaffold matrix. When testing different concentrations of CPO, we found that 0.25wt.% concentration produced the most desirable results; these bioscaffolds generated biologically relevant concentrations of oxygen[17,27] over 21 days while also producing the lowest amount of ROS compared bioscaffolds which incorporated higher concentrations of CPO. Furthermore, 21 days is long enough for islets to establish their own blood supply following transplantation, which has been reported to take on average 14 days.[53,54] Following seeding of islets into cryogel-0.25wt.%CPO bioscaffolds, islets demonstrated significantly increased viability and function which was also confirmed using computational modelling as well as confocal microscopy which both demonstrated the islet core remained viable and functional only when oxygen was present in the microenvironment.

Our results showed that incorporation of 0.25wt.%CPO within our bioscaffolds resulted in the highest degree of islet survival and function when compared to cryogel bioscaffolds with higher concentrations of CPO (i.e. 0.5wt.% and 1wt.%CPO). By increasing the concentration of CPO within our cryogel bioscaffolds, we were able to increase the amount of oxygen generated, however, this did not correlate with improved islet survival and function. One reason is at higher concentrations of CPO, there was an increased production of ROS which has a detrimental effect on islets. This is further supported by our data which demonstrated that islet function and viability was reduced in direct correlation to the concentration of ROS to which they were exposed (Figure S4).

When our cryogel-0.25wt.%CPO bioscaffolds were translated *in vivo* into diabetic animals, they reversed hyperglycemia and restored glycemic control during basal conditions while also improving dynamic responses to glucose challenges. In addition, the EFP from these mice contained a significantly higher amount of insulin compared to mice transplanted with islets only or those seeded into bioscaffolds made from cryogel alone thereby indicating that there was a higher amount of viable and functional β cells within these animals. Furthermore, within the EFP, we also noted an up-regulation of MIP-1α and -β,[55] IP-10,[56] and IL-6,[57] (i.e. cytokines which promote angiogenesis), and down-regulation of IL-9,[58] LIX,[59] and TNF-α,[60] (i.e. cytokines which demonstrate pro-inflammatory activity)

when compared to the control EFP in which islets alone were transplanted. This was further supported by our data which showed decreased inflammation (no TNFα staining) in the histological sections of the EFP containing our cryogel-0.25wt.%CPO bioscaffolds. When we compared the EFP from animals which received cryogel-0.25wt.%CPO bioscaffolds to those which had cryogel alone bioscaffolds, there was a significant increase in the expression of IL-22[61] (i.e. a cytokine which promotes angiogenesis), LIF[62] (i.e. a cytokine which regulates microvessel density), and a significant decrease in expression of IL28,[63] IL-17α,[64] and TNF-α[60] (i.e. pro-inflammatory cytokines). However, the decreased efficiency of islet transplantation in our control experiments (i.e. islets alone transplanted into the EFP) compared to previous studies[52,65,66] can be attributed to (i) the use of 500 islets with islet diameters in the range of 50–150μm – this is less than 500 islet equivalents or IEQ used in previous studies[52,65,66] (one IEQ is considered equivalent to an islet with a diameter of 150μm) and (ii) our animals exhibited a higher initial blood glucose at the day of transplantation (i.e. 538±25mg/dL) when compared to the above mentioned studies (i.e. 250mg/dL or 350mg/dL or 500mg/dL)[52,65,66] – this would mean that our animals had a greater degree of dysglycemia and hence are much more dependent on the success of their islet transplant.

In addition, we assessed the effect of oxygen release from our cryogel-0.25wt.%CPO bioscaffolds on the level of HIF1 (i.e. a cellular marker of hypoxia) expression within the EFPs of diabetic mice transplanted with islets seeded in our bioscaffolds. Our results showed a lower expression of HIF1α protein (i.e. a subunit of HIF1) in EFPs transplanted with islets seeded into our cryogel-0.25wt.%CPO bioscaffolds. HIF1 is known as the key regulator of hypoxia-induced gene expression, and reports suggest that induction of HIF1α predicts adverse transplant outcomes[67]. Hence, our results suggest that the oxygen released from our cryogel-CPO bioscaffolds can alter the HIF1α expression within the transplantation site (i.e. the EFP in our study) which may have an important role in protecting β cells within islets from hypoxia induced death following their transplantation.

The biocompatibility of biomaterials has been shown to be critical for the safety and integrity of long-term implants.[68] In contrast with synthetic polymer bioscaffolds, which can often lead to intense inflammatory reactions manifested by deposition of significant amounts of fibrotic tissue at the interface of the bioscaffold with the surrounding tissue[9] and long-term dwelling of macrophages,[9] our collagen based cryogel bioscaffold did not induce any intense foreign-body reaction in the immediate (30 days) or long (6 month) term. Furthermore, animals which received bioscaffolds did not demonstrate any change in their blood panels with all results remaining within the normal range.

The in vitro biodegradability rate was also shown to be sufficiently low such that bioscaffolds would be expected to last for >5 years, thereby providing a stable matrix to accommodate islets until they are fully engrafted into the host tissue. Nevertheless, the results obtained from our in vitro biodegradability studies need to be interpreted with caution as they are not completely representative of the in vivo environment.[69,70] Indeed, the in vivo biodegradation rate will be strongly dependent not only on the location of the bioscaffold, but also the surrounding blood flow, oxygen supply, pH values as well as the amount of water and ion content in the local microenvironment.[71] Also, given that a drop

in pH occurs post-surgery, this can lead to a short-term increase in the biodegradation rate and the deposition of biodegradation products on the implant's surfaces,[70] which, in turn, can then decrease the overall biodegradation rate. Hence, although our results predict >5 years stability of our bioscaffolds, long-term *in vivo* biodegradability studies will need to be undertaken for full evaluation. However, if the body rejects the implant, a localized inflammatory response will occur. In that case, a quicker biodegradability would be beneficial. The biodegradability of our bioscaffolds can be increased by decreasing the concentration of the collagen matrix (e.g. <3% (wt./vol.)) and EDC/NHS cross-linker (e.g. <15mM NHS and 30mM EDC). Quicker biodegradability however can potentially have a negative effect on the mechanical properties and structural integrity of bioscaffolds which also need to be considered. Although several cellular and molecular factors have been shown to be involved in collagen biodegradation, the exact mechanisms are largely unknown.[72] Given that our in vitro biodegradation test was performed in PBS solution, surface biodegradation is therefore thought to be the predominant mechanism underlying our bioscaffold biodegradation.

Current clinical practice for islet transplantation involves islets being infused into the liver, thereby rendering them irretrievable.[73] While this site cannot accommodate the implantation of a 3D bioscaffold, other sites such as the omentum are being explored given it has (i) a well vascularized surface area,[26] (ii) the ability to accommodate bioscaffolds and (iii) the ability to enable retrieval of bioscaffolds should something adverse happen. Indeed, human clinical trials are already underway examining the feasibility of the omentum as a site for islet transplantation.[26] In small animals, the EFP (i.e. the site used in our study) is a surrogate site for the omentum in humans.[26,74,75] In our biocompatibility study, we also examined the subcutaneous space as a site for our bioscaffold given it can be easily accessed in patients and thus has the potential to be widely adopted as a space for bioscaffold implantation with minimal intervention; future research will aim to examine this site with our cryogel-0.25wt.%CPO bioscaffold in diabetic mice. In humans, islets are typically given at 5,000 islets per kg (i.e. a weight based approach) which, on average, translates to approximately 350,000–450,000 islets.[76] By changing the synthesis molds, our current bioscaffold can be easily scaled to 100 cm^3, which we have calculated can accommodate the required number of islets required for humans, thereby confirming our bioscaffold can be clinically translated. Finally, our cryogel-0.25wt.%CPO bioscaffold is composed of two components: collagen and CPO. Collagen is FDA-approved and Phase 2 clinical trials are already underway using this material in bioscaffolds for other applications (i.e. ClinicalTrials.gov; Identifier: NCT03613090). CPO is also a biocompatible material that has been extensively used as an oxygen-generating biomaterial,[77–79] however, it does produce ROS which can have harmful effects. Similar to our study, Sheikh et al[41] reported the development of an oxygen-releasing antioxidant polyurethane cryogel scaffold (PUAO-CPO) for sustained oxygen delivery which improved the function of its cellular cargo. In their study, the PUAO-CPO bioscaffold was able to both attenuate ROS while producing oxygen in a sustained manner, thereby sustaining H9C2 cardiomyoblast cells under hypoxic conditions. Given there is no published literature, to our knowledge, examining the effects of ROS in either the subcutaneous or adipose tissue compartments at the levels generated by our cryogel-0.25wt.%CPO bioscaffold, future studies examine this in more detail. In

addition, we will assess the ability of antioxidants that can be incorporated in our cryogel-CPO bioscaffold in modulating the amount and effect of any ROS produced from CPO.

In summary, our cryogel-0.25wt.%CPO bioscaffold (i) provides a safe and stable engineering microenvironment for islets; (ii) protects islets; (iii) is able to generate oxygen in a sustained and controlled manner in the short term, thereby improving islet survival and function until they can engraft and establish their own vascular supply; and (iv) can be implanted at extra-hepatic sites such as the omentum or even in the subcutaneous tissues. Future work will focus on the long-term function (e.g. > 6 months) of our cryogel-0.25wt.%CPO bioscaffold for islet transplantation in diabetic animal models. Future work can also further optimize our cryogel-0.25wt.%CPO bioscaffold with the incorporation of ECM molecules[44,75,80] or growth factors. [81,82] ECM molecules or growth factors can be incorporated into our cryogel-0.25wt.%CPO bioscaffold using a polydopamine coating. As polydopamine has repeating 3,4-dihydroxy-L-phenylalanine-lysine (DOPA-K) motifs, it has strong adsorption through covalent bonding and intermolecular interactions.[83] Hence, polydopamine coatings could serve as the interface to enable our bioscaffold to be coated with ECM molecules or growth factors.[84] In addition, given our STZ-induced diabetic animal models does not fully mimic T1D, given the lack of a background autoimmune component, so future work can examine responses in NOD mice over longer durations.

Supplementary Material

Refer to Web version on PubMed Central for supplementary material.

ACKNOWLEDGEMENTS

This work was supported by the NIDDK/NIH (R01DK119293 and P30DK116074), the Akiko Yamzaki and Jerry Yang Faculty Scholar Fund in Pediatric Translational Medicine and the Stanford Maternal and Child Health Research Institute, and the SIR Foundation Ring Development Grant. This work was also supported by the Stanford Nano Shared Facilities (SNSF) grant (1161726-146-DAARZ), as part of the grant supported by the National Science Foundation grant (ECCS-1542152), and the Stanford Neuroscience Microscopy Service grant (NIH NS069375). The authors also wish to acknowledge Dr. Mujib Ullah for performing Western blot analysis.

REFERENCES

[1]. Barnett BP, Arepally A, Karmarkar PV, Qian D, Gilson WD, Walczak P, Howland V, Lawler L, Lauzon C, Stuber M, Kraitchman DL, Bulte JWM, Nat. Med 2007, 13, 986. [PubMed: 17660829]

[2]. Scharp DW, Marchetti P, Encapsulated islets for diabetes therapy: History, current progress, and critical issues requiring solution. Adv. Drug Deliv. Rev 2014, 67–68, 35–73.

[3]. Liao SW, Rawson J, Omori K, Ishiyama K, Mozhdehi D, Oancea AR, Ito T, Guan Z, Mullen Y, Biomaterials 2013, 34, 3984. [PubMed: 23465491]

[4]. Kheradmand T, Wang S, Gibly RF, Zhang X, Holland S, Tasch J, Graham JG, Kaufman DB, Miller SD, Shea LD, Luo X, Biomaterials 2011, 32, 4517. [PubMed: 21458857]

[5]. Pedraza E, Brady AC, Fraker CA, Molano RD, Sukert S, Berman DM, Kenyon NS, Pileggi A, Ricordi C, Stabler CL, Cell Transplant. 2013, 22, 1123. [PubMed: 23031502]

[6]. Smink AM, Hertsig DT, Schwab L, Van Apeldoorn AA, De Koning E, Faas MM, De Haan BJ, De Vos P, Ann. Surg 2017, 266, 149. [PubMed: 27429018]

[7]. Buitinga M, Assen F, Hanegraaf M, Wieringa P, Hilderink J, Moroni L, Truckenmüller R, van Blitterswijk C, Römer GW, Carlotti F, de Koning E, Karperien M, van Apeldoorn A, Biomaterials 2017, 135, 10. [PubMed: 28478326]

[8]. Stendahl JC, Wang LJ, Chow LW, Kaufman DB, Stupp SI, Transplantation 2008, 86, 478. [PubMed: 18698254]

[9]. Wang X, Wang K, Zhang W, Qiang M, Luo Y, Biomaterials 2017, 138, 80. [PubMed: 28554010]

[10]. Bhat S, Tripathi A, Kumar A, Soc JR. Interface 2011, 8, 540. [PubMed: 20943683]

[11]. Carlsson PO, Liss P, Andersson A, Jansson L, Diabetes 1998, 47, 1027. [PubMed: 9648824]

[12]. Lee CH, Singla A, Lee Y, Int. J. Pharm 2001, 221, 1. [PubMed: 11397563]

[13]. Rodrigues SC, Salgado CL, Sahu A, Garcia MP, Fernandes MH, Monteiro FJ, J. Biomed. Mater. Res. - Part A 2013, 101 A, 1080.

[14]. Hlavaty KA, Gibly RF, Zhang X, Rives CB, Graham JG, Lowe WL, Luo X, Shea LD, Am. J. Transplant 2014, 14, 1523. [PubMed: 24909237]

[15]. Liu JMH, Zhang J, Zhang X, Hlavaty KA, Ricci CF, Leonard JN, Shea LD, Gower RM, Biomaterials 2016, 80, 11. [PubMed: 26701143]

[16]. Daoud JT, Petropavlovskaia MS, Patapas JM, Degrandpré CE, DiRaddo RW, Rosenberg L, Tabrizian M, Biomaterials 2011, 32, 1536. [PubMed: 21093908]

[17]. Coronel MM, Geusz R, Stabler CL, Biomaterials 2017, 129, 139. [PubMed: 28342320]

[18]. Ludwig B, Reichel A, Steffen A, Zimerman B, Schally AV, Block NL, Colton CK, Ludwig S, Kersting S, Bonifacio E, Solimena M, Gendler Z, Rotem A, Barkai U, Bornstein SR, Proc. Natl. Acad. Sci 2013, 110, 19054. [PubMed: 24167261]

[19]. Razavi M, Hu S, Thakor AS, J. Biomed. Mater. Res. - Part A 2018, 106, 2213.

[20]. Pedraza E, Coronel MM, Fraker CA, Ricordi C, Stabler CL, Proc. Natl. Acad. Sci 2012, 109, 4245. [PubMed: 22371586]

[21]. Northup A, Cassidy D, J. Hazard. Mater 2008, 152, 1164. [PubMed: 17804164]

[22]. Acharya JD, Ghaskadbi SS, Islets and their antioxidant defense. Islets 2010, 2, 225–235. [PubMed: 21099317]

[23]. Maechler P, Jornot L, Wollheim CB, J. Biol. Chem 1999, 274, 27905. [PubMed: 10488138]

[24]. Tang J, Zhang JH, Life Sci 2000, 68, 475. [PubMed: 11205896]

[25]. Wang K, Wang X, Han C, Chen L, Luo Y, J. Vis. Exp 2017.

[26]. Schmidt C, Nat. Biotechnol 2017, 35, 8. [PubMed: 28072777]

[27]. Buchwald P, Theor. Biol. Med. Model 2011, 8.

[28]. Buchwald P, Tamayo-Garcia A, Manzoli V, Tomei AA, Stabler CL, Biotechnol. Bioeng 2018, 115, 232. [PubMed: 28865118]

[29]. Fournier RL, Basic Transport Phenomena in Biomedical Engineering, 3rd ed.; CRC Press, 2011.

[30]. Carlsson PO, Palm F, Andersson A, Liss P, Diabetes 2001, 50, 489. [PubMed: 11246867]

[31]. Komatsu H, Rawson J, Barriga A, Gonzalez N, Mendez D, Li J, Omori K, Kandeel F, Mullen Y, Am. J. Transplant 2018.

[32]. Bochenek MA, Veiseh O, Vegas AJ, McGarrigle JJ, Qi M, Marchese E, Omami M, Doloff JC, Mendoza-Elias J, Nourmohammadzadeh M, Khan A, Yeh CC, Xing Y, Isa D, Ghani S, Li J, Landry C, Bader AR, Olejnik K, Chen M, Hollister-Lock J, Wang Y, Greiner DL, Weir GC, Strand BL, Rokstad AMA, Lacik I, Langer R, Anderson DG, Oberholzer J, Nat. Biomed. Eng 2018, 2, 810. [PubMed: 30873298]

[33]. Rodriguez-Diaz R, Molano RD, Weitz JR, Abdulreda MH, Berman DM, Leibiger B, Leibiger IB, Kenyon NS, Ricordi C, Pileggi A, Caicedo A, Berggren PO, Cell Metab. 2018, 27, 549. [PubMed: 29514065]

[34]. Ullah M, Sun Z, Journals Gerontol. Ser. A 2019, 74, 1396.

[35]. Otto GP, Rathkolb B, Oestereicher MA, Lengger CJ, Moerth C, Micklich K, Fuchs H, Gailus-Durner V, Wolf E, Hrabě de Angelis M, J. Am. Assoc. Lab. Anim. Sci 2016, 55, 375. [PubMed: 27423143]

[36]. Boehm O, Zur B, Koch A, Tran N, Freyenhagen R, Hartmann M, Zacharowski K, Biol. Chem 2007, 388, 547. [PubMed: 17516851]

[37]. Olsson R, Carlsson PO, Diabetes 2011, 60, 2068. [PubMed: 21788581]

[38]. Lifson N, Lassa CV, Dixit PK, Am. J. Physiol. Metab 2017, 249, E43.

[39]. Razavi M, Hu S, Thakor AS, J. Biomed. Mater. Res. - Part A 2018, 106, 2213.

[40]. Morini S, Brown ML, Cicalese L, Elias G, Carotti S, Gaudio E, Rastellini C, J. Anat 2007, 210, 565. [PubMed: 17394557]

[41]. Shiekh PA, Singh A, Kumar A, ACS Appl. Mater. Interfaces 2018, 10, 18458. [PubMed: 29737151]

[42]. Jia W, Tang H, Wu J, Hou X, Chen B, Chen W, Zhao Y, Shi C, Zhou F, Yu W, Huang S, Ye G, Dai J, Biomaterials 2015, 69, 45. [PubMed: 26280949]

[43]. Irving-Rodgers HF, Choong FJ, Hummitzsch K, Parish CR, Rodgers RJ, Simeonovic CJ, Cell Transplant. 2014, 23, 59. [PubMed: 23211522]

[44]. Salvay DM, Rives CB, Zhang X, Chen F, Kaufman DB, Lowe WL, Shea LD, Transplantation 2008, 85, 1456. [PubMed: 18497687]

[45]. Abualhassan N, Sapozhnikov L, Pawlick RL, Kahana M, Pepper AR, Bruni A, Gala-Lopez B, Kin T, Mitrani E, Shapiro AMJ, PLoS One 2016, 11.

[46]. Sionov RV, Finesilver G, Sapozhnikov L, Soroker A, Zlotkin-Rivkin E, Saad Y, Kahana M, Bodaker M, Alpert E, Mitrani E, Tissue Eng. Part A 2015, 21, 2691. [PubMed: 26416226]

[47]. Kumar A, Srivastava A, Nat. Protoc 2010, 5, 1737. [PubMed: 21030950]

[48]. Kumar A, Mishra R, Reinwald Y, Bhat S, Mater. Today 2010, 13, 42.

[49]. Lehmann R, Zuellig RA, Kugelmeier P, Baenninger PB, Moritz W, Perren A, Clavien PA, Weber M, Spinas GA, Diabetes 2007, 56, 594. [PubMed: 17327426]

[50]. Davalli AM, Scaglia L, Zangen DH, Hollister J, Bonner-Weir S, Weir GC, Diabetes 1996, 45, 1161. [PubMed: 8772716]

[51]. Carlsson PO, Liss P, Andersson A, Jansson L, Diabetes 1998, 47, 1027. [PubMed: 9648824]

[52]. Jiang K, Weaver JD, Li Y, Chen X, Liang J, Stabler CL, Biomaterials 2017, 114, 71. [PubMed: 27846404]

[53]. Calderari S, Chougnet C, Clemessy M, Kempf H, Corvol P, Larger E, PLoS One 2012, 7.

[54]. Weiss JF, Landauer MR, Toxicology 2003, 189, 1. [PubMed: 12821279]

[55]. Liao Y-Y, Tsai H-C, Chou P-Y, Wang S-W, Chen H-T, Lin Y-M, Chiang I-P, Chang T-M, Hsu S-K, Chou M-C, Tang C-H, Fong Y-C, Oncotarget 2015, 7.

[56]. Liu M, Guo S, Hibbert JM, Jain V, Singh N, Wilson NO, Stiles JK, CXCL10/IP-10 in infectious diseases pathogenesis and potential therapeutic implications. Cytokine Growth Factor Rev. 2011, 22, 121–130. [PubMed: 21802343]

[57]. Huang SP, Wu MS, Shun CT, Wang HP, Lin MT, Kuo ML, Lin JT, J. Biomed. Sci 2004, 11, 517. [PubMed: 15153787]

[58]. Goswami R, Kaplan MH, J. Immunol 2011, 186, 3283. [PubMed: 21368237]

[59]. Chandrasekar B, Melby PC, Sarau HM, Raveendran M, Perla RP, Marelli-Berg FM, Dulin NO, Singh IS, J. Biol. Chem 2003, 278, 4675. [PubMed: 12468547]

[60]. Dinarello CA, Chest 2000, 118, 503. [PubMed: 10936147]

[61]. Protopsaltis NJ, Liang W, Nudleman E, Ferrara N, Angiogenesis 2018, 0, 0.

[62]. Kubota Y, Hirashima M, Kishi K, Stewart CL, Suda T, J. Clin. Invest 2008, 118, 2393. [PubMed: 18521186]

[63]. Lee SJ, Lee EJ, Kim SK, Jeong P, Cho YH, Yun SJ, Kim S, Kim GY, Choi YH, Cha EJ, Kim WJ, Moon SK, PLoS One 2012, 7.

[64]. Hot A, Lenief V, Miossec P, Ann. Rheum. Dis 2012, 71, 768. [PubMed: 22258491]

[65]. Blomeier H, Zhang X, Rives C, Brissova M, Hughes E, Baker M, Powers AC, Kaufman DB, Shea LD, Lowe WL, Transplantation 2006, 82, 452. [PubMed: 16926587]

[66]. Gibly RF, Zhang X, Graham ML, Hering BJ, Kaufman DB, Lowe WL, Shea LD, Biomaterials 2011, 32, 9677. [PubMed: 21959005]

[67]. Stokes RA, Cheng K, Deters N, Lau SM, Hawthorne WJ, O'Connell PJ, Stolp J, Grey S, Loudovaris T, Kay TW, Thomas HE, Gonzalez FJ, Gunton JE, Cell Transplant. 2013, 22, 259.

[68]. Chang R, Faleo G, Russ HA, Parent AV, Elledge SK, Bernards DA, Allen JL, Villanueva K, Hebrok M, Tang Q, Desai TA, ACS Nano 2017, 11, 7747. [PubMed: 28763191]

[69]. Walker J, Shadanbaz S, Kirkland NT, Stace E, Woodfield T, Staiger MP, Dias GJ, J. Biomed. Mater. Res. - Part B Appl. Biomater 2012, 100 B, 1134.

[70]. Witte F, Fischer J, Nellesen J, Crostack H-A, Kaese V, Pisch A, Beckmann F, Windhagen H, Biomaterials 2006, 27, 1013. [PubMed: 16122786]

[71]. Reifenrath J, Marten A-K, Angrisani N, Eifler R, Weizbauer A, Biomed. Mater 2015, 10, 045021. [PubMed: 26267552]

[72]. Gross J, Cell Biol. Extracell. Matrix 2011, 217.

[73]. Shapiro AMJ, Ricordi C, Hering BJ, Auchincloss H, Lindblad R, Robertson RP, Secchi A, Brendel MD, Berney T, Brennan DC, Cagliero E, Alejandro R, Ryan EA, DiMercurio B, Morel P, Polonsky KS, Reems J-A, Bretzel RG, Bertuzzi F, Froud T, Kandaswamy R, Sutherland DER, Eisenbarth G, Segal M, Preiksaitis J, Korbutt GS, Barton FB, Viviano L, Seyfert-Margolis V, Bluestone J, Lakey JRT, Engl N. J. Med 2006.

[74]. Berman DM, Molano RD, Fotino C, Ulissi U, Gimeno J, Mendez AJ, Kenyon NM, Kenyon NS, Andrews DM, Ricordi C, Pileggi A, Diabetes 2016, 65, 1350. [PubMed: 26916086]

[75]. Gibly RF, Zhang X, Lowe WL, Shea LD, Cell Transplant. 2013, 22, 811. [PubMed: 22507300]

[76]. McCall M, James Shapiro AM, Cold Spring Harb. Perspect. Med 2012, 2.

[77]. Camci-Unal G, Alemdar N, Annabi N, Khademhosseini A, Polym. Int 2013, 62, 843. [PubMed: 23853426]

[78]. McQuilling JP, Opara EC, In Methods in Molecular Biology; 2017.

[79]. Gholipourmalekabadi M, Zhao S, Harrison BS, Mozafari M, Seifalian AM, Oxygen-Generating Biomaterials: A New, Viable Paradigm for Tissue Engineering? Trends Biotechnol. 2016, 34, 1010–1021. [PubMed: 27325423]

[80]. Yap WT, Salvay DM, Silliman MA, Zhang X, Bannon ZG, Kaufman DB, Lowe WL, Shea LD, Tissue Eng. Part A 2013, 19, 2361. [PubMed: 23713524]

[81]. Brady A-C, Martino MM, Pedraza E, Sukert S, Pileggi A, Ricordi C, Hubbell JA, Stabler CL, Tissue Eng. Part A 2013, 19, 2544. [PubMed: 23790218]

[82]. Vernon RB, Preisinger A, Gooden MD, D'Amico LA, Yue BB, Bollyky PL, Kuhr CS, Hefty TR, Nepom GT, Gebe JA, Cell Transplant. 2012, 21, 2099. [PubMed: 23231959]

[83]. Lee H, Dellatore SM, Miller WM, Messersmith PB, Science (80-.) 2007, 318, 426.

[84]. Shin YM, Bin Lee Y, Kim SJ, Kang JK, Park JC, Jang W, Shin H, Biomacromolecules 2012, 13, 2020. [PubMed: 22617001]

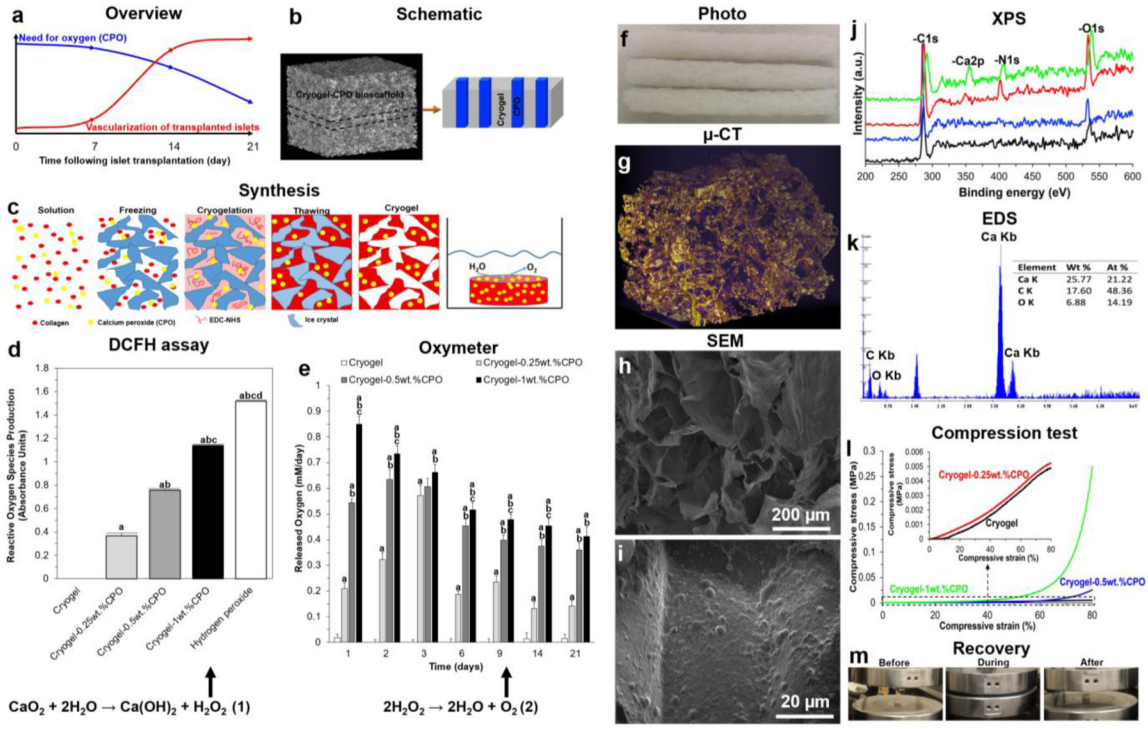

Figure 1. Bioscaffold synthesis and characterization:

(a) Schematic representation showing the temporal relationship between the oxygen requirement for transplanted islets over the first 3 weeks following their engraftment and the time taken for them to establish their own blood supply; **(b)** Schematic illustration of our cryogel-CPO bioscaffold and **(c)** the preparation of cryogel-CPO bioscaffolds: Collagen was swollen overnight in HCl at 4°C. The collagen dispersion was then homogenized and centrifuged. CPO (concentrations of 0.25, 0.5 and 1wt.%) was then mixed with the collagen slurry. After transferring the collagen-CPO slurry to a mold, NHS/EDC was added (depicted as the solution); the molds were kept in a freezer at −20°C for 24h (depicted as the freezing) to complete the crosslinking process (depicted as the cryogelation). Next, bioscaffolds were thawed at room temperature (depicted as the thawing). Following exposure of the synthesized cryogel-CPO bioscaffold to water, oxygen was generated and diffused out from the bioscaffold via a hydrolytic reaction; **(d)** The amount of oxygen released from cryogel alone and cryogel-CPO bioscaffolds incubated in PBS up to 21 days; and **(e)** ROS produced from cryogel, cryogel-CPO bioscaffolds and hydrogen peroxide (as control group) incubated in culture medium for 24 h; Bioscaffold structural analysis: **(f)** Photographs of cryogel-CPO bioscaffolds showing the macrostructure of bioscaffolds; **(g)** Reconstructed μ-CT images of a cryogel-CPO bioscaffold; yellow areas show the bioscaffold material and the purple areas refer to the void space; **(h-i)** SEM images of a cryogel-CPO bioscaffold showing the existence of (h) macropores and (i) CPO particles throughout the bioscaffold. Bioscaffold chemical analysis: **(j)** XPS spectra and **(k)** EDS analysis showing the four elements of C, O, N and Ca corresponding to the molecular formula which are basic elements of collagen and CPO; Bioscaffold mechanical analysis: **(l)** Compression stress–strain curves of bioscaffolds in the wet state; **(m)** The recovery of bioscaffolds to their original shape after removing the

load in the compression test showing their mechanical flexibility; Measurement of oxygen release and ROS production in bioscaffolds:

Significant differences:

[a]P<0.05: cryogel vs. cryogel-0.25, 0.5 and 1wt.% CPO bioscaffolds and hydrogen peroxide; [b]P<0.05: cryogel-0.25wt.%CPO vs. cryogel-0.5 and 1wt.% CPO bioscaffolds and hydrogen peroxide; [c]P<0.05: cryogel-0.5wt.%CPO vs. cryogel-1wt.% CPO bioscaffolds and hydrogen peroxide; [d]P<0.05: cryogel-1wt.% vs. hydrogen peroxide. (One-way ANOVA post-hoc Tukey Test).

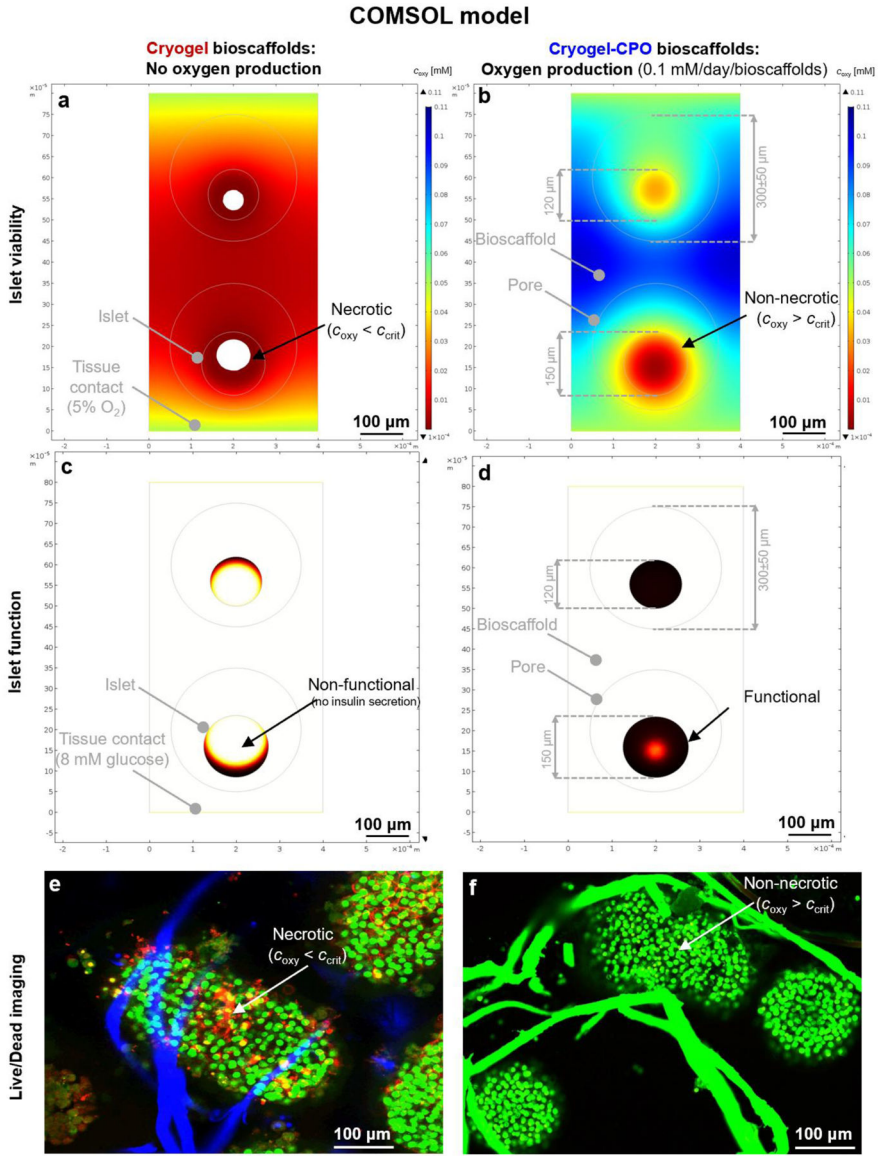

Figure 2. Computational model-calculated oxygen concentrations and insulin secretion rates: **(a,b)** Oxygen concentration and **(c,d)** insulin secretion rates for two islets with d = 120 & 150 µm seeded into cryogel-0.25wt.%CPO bioscaffolds that produce oxygen (0.1 mM/day/bioscaffold ≈ 0.01 M/m^3/s) **(a,c)**; or not (cryogel bioscaffolds as control) **(b,d)**. Data are shown at 8mM glucose for bioscaffolds with pore sizes of 300µm placed in normoxic tissue (oxygen 5% ≈ 0.05 mM) with symmetry conditions assumed at the left and right margins. Oxygen concentrations are color-coded from blue for high to red for low with white indicating levels that are below the critical concentration of oxygen (c_{oxy} < c_{crit}) for islet survival. Insulin secretion rates per unit volume within the islets are shown color-coded from black for high to white for zero with white indicating levels that are below the critical concentration of insulin ($c_{insulin}$ < c_{crit}) for islet function; **(e, f)** Experimental data showing the higher viability of islets seeded into cryogel-0.25wt.%CPO bioscaffolds **(f)** compared to

cryogel alone bioscaffolds **(e)** at day 7. Green = live cells, Red = Dead cells; Blue tubes = cryogel alone bioscaffold; Green tubes = cryogel-0.25 wt.%CPO bioscaffolds.

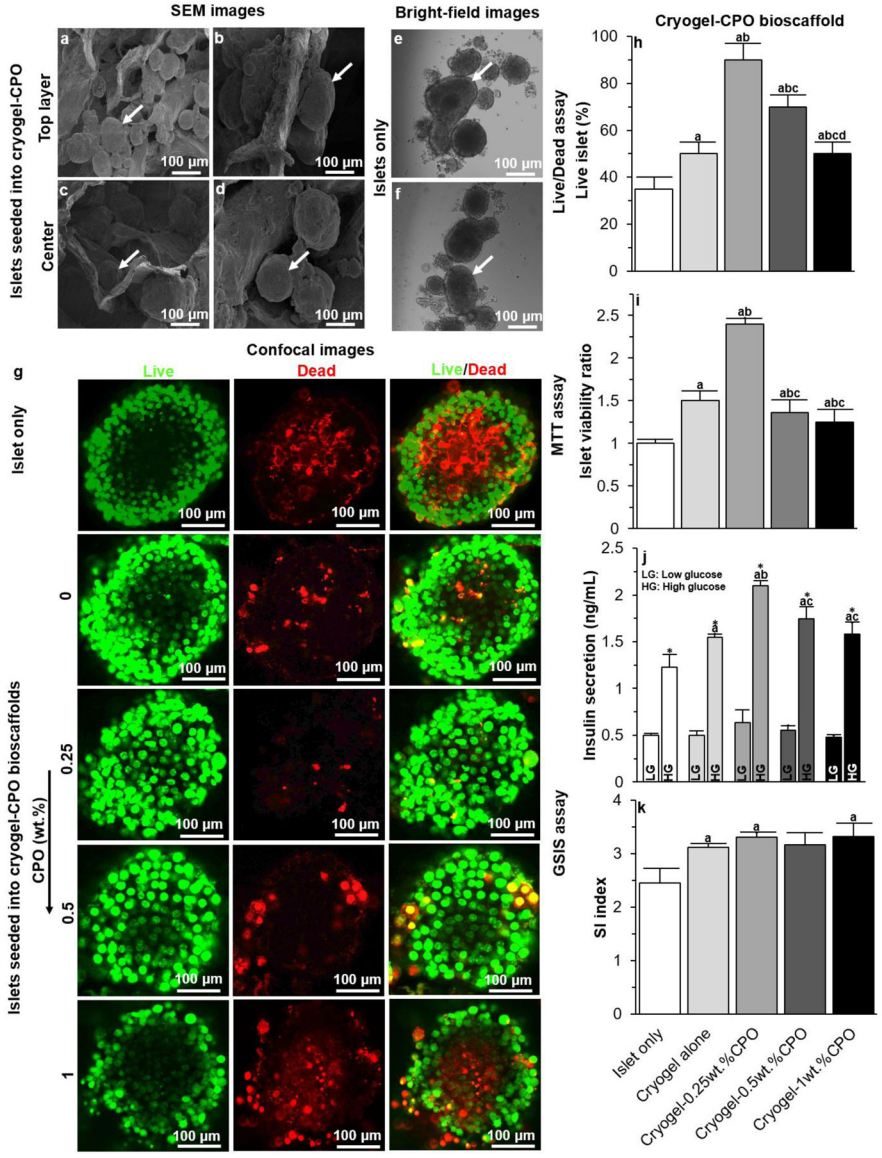

Figure 3. Bioscaffold interactions with pancreatic islets in vitro:

(a-d) SEM images of **(a-b)** the top surface and **(c-d)** center of our cryogel-0.25wt.%CPO bioscaffold seeded with islets; **(e-f)** Bright-field images of islets cultured in conventional culture plates; **(g)** Confocal images of islets cultured in culture plates or seeded into a cryogel alone bioscaffolds or cryogel-CPO bioscaffolds with 0.25, 0.5, and 1wt.%CPO at day 7. Green represents live cells and red represents dead cells; Results of **(h)** Live/Dead, **(i)** MTT, and **(j-k)** GSIS assays for islet only and islets seeded into cryogel bioscaffolds without, and with CPO, at day 7.

Significant differences:

(h-k) [a]P<0.05: islets only vs. cryogel and cryogel-0.25, 0.5 and 1wt.% CPO bioscaffolds; [b]P<0.05: cryogel bioscaffolds vs. cryogel-0.25, 0.5 and 1wt.% CPO bioscaffolds; [c]P<0.05: cryogel-0.25wt.% bioscaffolds vs. cryogel-0.5 and 1wt.% CPO bioscaffolds; [d]P<0.05:

cryogel-0.5wt.% bioscaffolds vs. cryogel-1wt.% CPO bioscaffolds; * Low glucose (LG) vs. high glucose (HG).

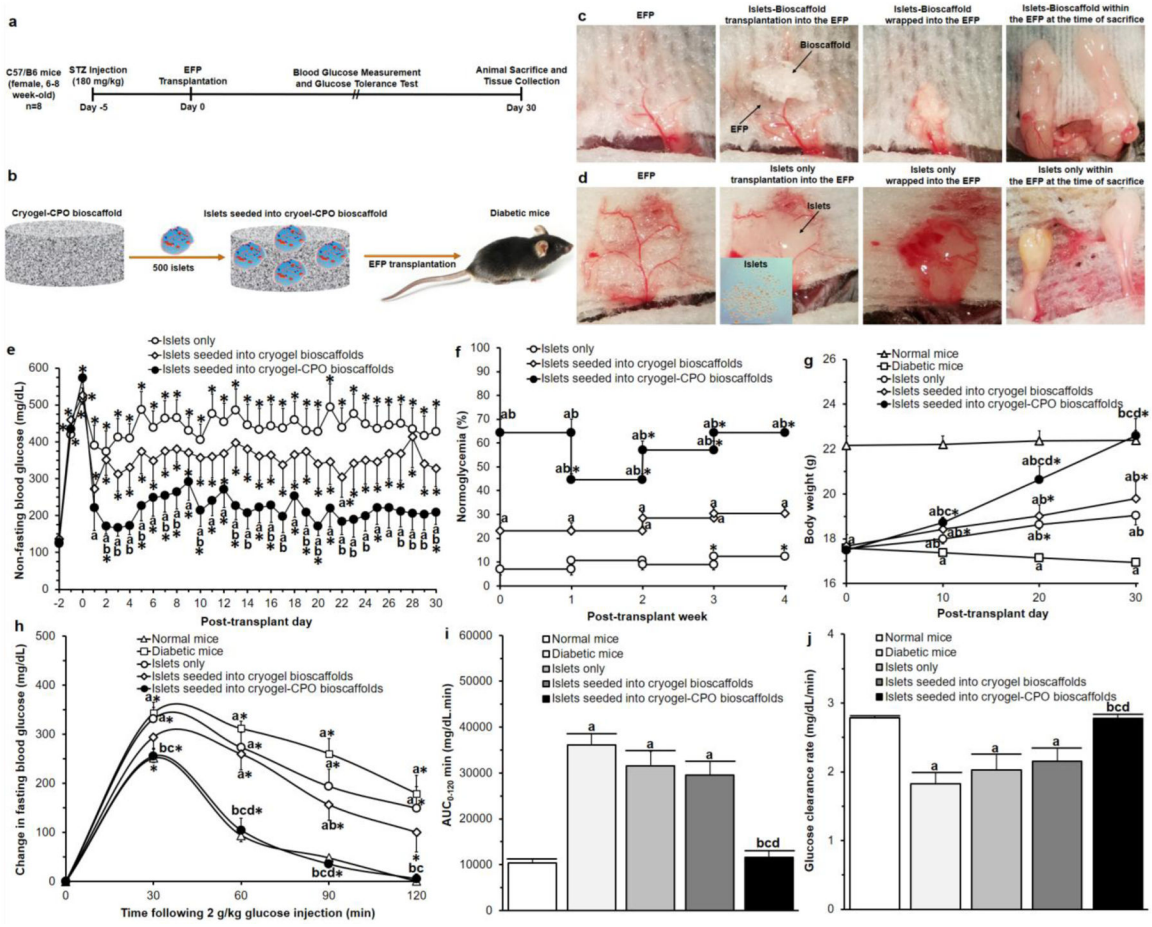

Figure 4. Bioscaffold interactions with pancreatic islets in vivo:

(a) Experimental details of our *in vivo* experiment; **(b)** Schematic representation of our bioscaffold transplantation in the EFP; Photographs of the transplantation procedure of **(c)** islets seeded into cryogel-0.25wt.%CPO and **(d)** islets only; Results of **(e)** non-fasting blood glucose measurements, **(f)** percentage of normoglycemia, **(g)** body weight, **(h)** IPGTT; Results of calculation of **(i)** area under the curve ($AUC_{0–120min}$) and **(j)** $slope_{30–60min}$ of IPGTT curves (i.e. glucose clearance rate).

Significant differences:

(e) [a]P<0.05: islets only vs. islets seeded into cryogel alone bioscaffolds and islets seeded into cryogel-0.25wt.%CPO bioscaffolds; [b]P<0.05: islets seeded into cryogel alone bioscaffolds vs. islets seeded into cryogel-0.25wt.%CPO bioscaffolds; *P<0.05: baseline (day −2) vs. all other time-points (Two-way ANOVA post-hoc Tukey Test).

(f) [a]P<0.05: islets only vs islets seeded into cryogel alone bioscaffolds and islets seeded into cryogel-0.25wt.%CPO bioscaffolds, [b]P<0.05: islets seeded into cryogel alone bioscaffolds *vs.* islets seeded into cryogel-0.25wt.%CPO bioscaffolds, *P<0.05: post-transplant week 0 *vs.* post-transplant week 1, 2, 3, and 4 (Two-way ANOVA post-hoc Tukey Test).

(g-j) [a]P<0.05: normal mice vs. diabetic mice, islets only, islets seeded into cryogel alone bioscaffolds, and islets seeded into cryogel-0.25wt.%CPO bioscaffolds; [b]P<0.05: diabetic mice vs. islets only, islets seeded into cryogel bioscaffolds, and islets seeded into

cryogel-0.25wt.%CPO bioscaffolds; [c]P<0.05: islets only vs. islets seeded into cryogel bioscaffolds, and islets seeded into cryogel-0.25wt.%CPO bioscaffolds; [d]P<0.05: islets seeded into cryogel bioscaffolds vs. islets seeded into cryogel-0.25wt.%CPO bioscaffolds; **(g)** *P<0.05: post-transplant day 0 vs. post-transplant day 10, 20, and 30, **(h)** *P<0.05: 0 min vs. 30, 60, 90 and 120 min (Two-way ANOVA post-hoc Tukey Test).

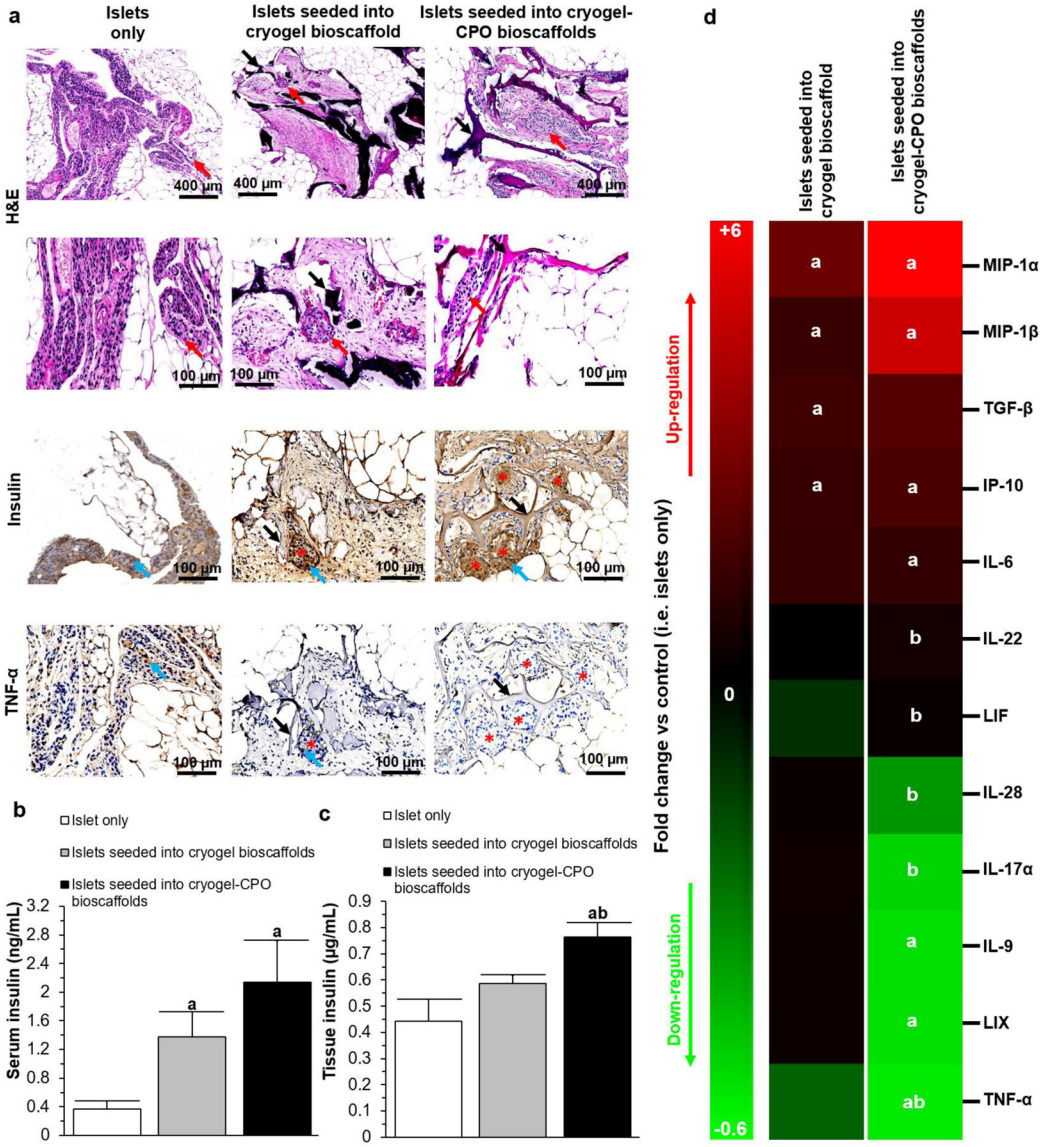

Figure 5. Histological and molecular analyses:

(a) Representative histological (H&E staining) and immunohistochemical images (insulin, and TNF-α staining) of the EFP containing islets only or islets seeded into cryogel alone and cryogel-0.25wt.%CPO bioscaffolds; H&E images: Red arrows=islets; immunohistochemical images: Black arrows= bioscaffolds, Red stars=islets, Blue arrows=positive (brown) staining; **(b-c)** The level of insulin within the **(b)** blood serum and **(c)** EFP; **(d)** Cytokines expression profile within the EFP tissue.

Significant differences:

[a]P<0.05: islets only vs. islets seeded into cryogel bioscaffolds and islets seeded into cryogel-0.25wt.%CPO bioscaffolds; [b]P<0.05: islets seeded into cryogel bioscaffolds vs. and islets seeded into cryogel-0.25wt.%CPO bioscaffolds. (One-way ANOVA post-hoc Tukey Test).

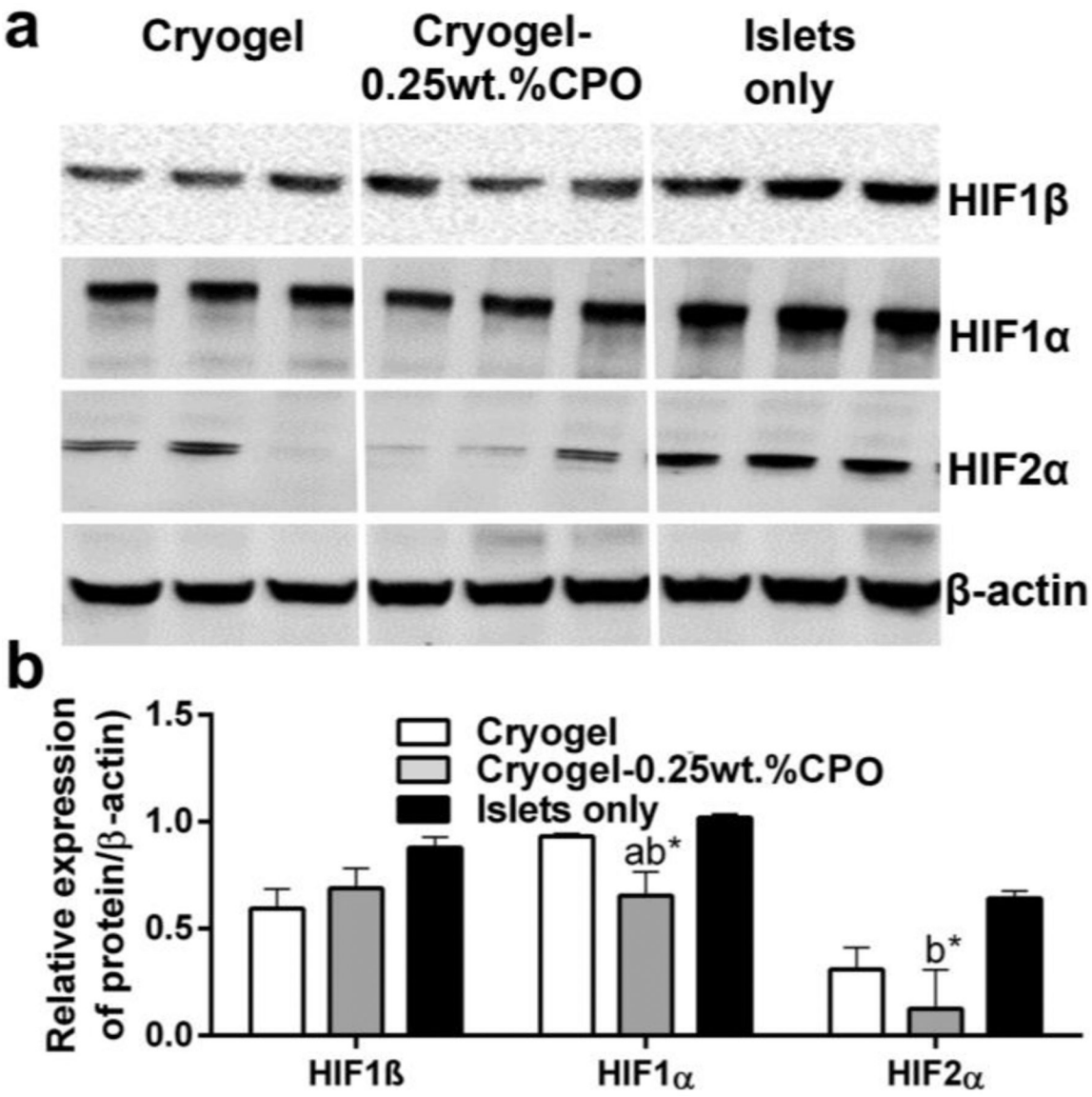

Figure 6. Assessment of HIF Expression;

(a) Western blot for HIF1β, HIF1α, HIF2α and β-actin. **(b)** Quantification of western blot. Significant differences:

[a]P<0.05: islets seeded into cryogel bioscaffolds vs. and islets seeded into cryogel-0.25wt.%CPO bioscaffolds; [b]P<0.05: islets only vs. islets seeded into cryogel bioscaffolds and islets seeded into cryogel-0.25wt.%CPO bioscaffolds; *P<0.05: islets only, islets seeded into cryogel bioscaffolds and islets seeded into cryogel-0.25wt.%CPO bioscaffolds vs control (i.e. β-actin).

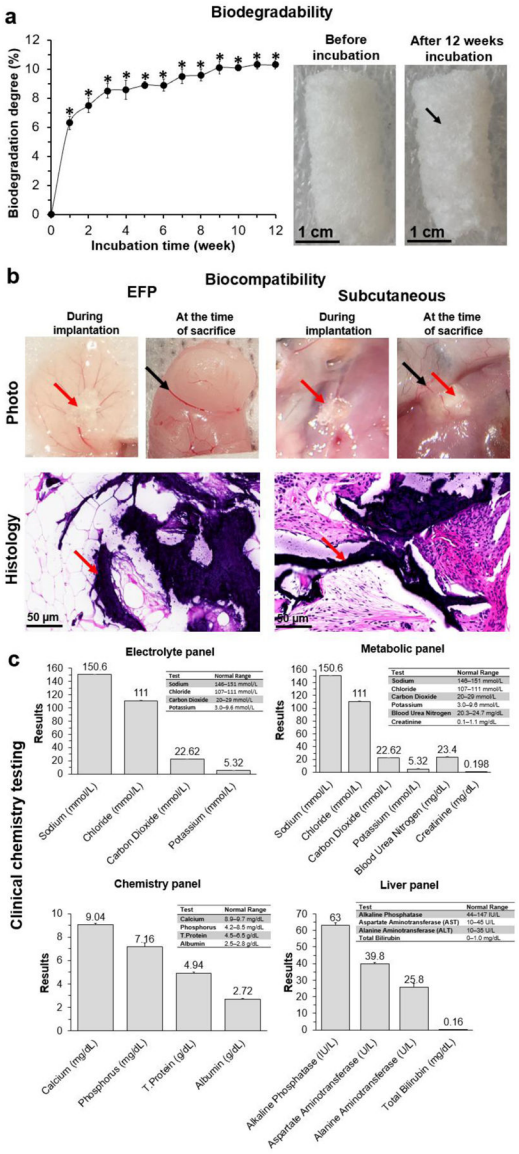

Figure 7. Bioscaffold biodegradability and biocompatibility:

(a) The biodegradation profile of cryogel-0.25wt.%CPO bioscaffolds incubated in PBS for 3 months; **(b)** Photographic, representative histological (H&E staining) of the EFP and subcutaneous tissue implanted with cryogel-0.25wt.%CPO bioscaffolds; Red arrow=bioscaffold; Black arrows=blood vessels (photographs); **(c)** Blood electrolyte, metabolic, chemistry, and liver panels from mice that had been implanted with cryogel-0.25wt.%CPO for 6 months. The normal range for each parameter is listed in a table in each of the four panels.